WARITH SCIENTIFIC JOURNAL OF ENGINEERING AND TECHNOLOGY 2026;2:71–88

Scan the QR to view the full-text article on the journal website

Potential Spatiotemporal Variability for Meteorological Drought in Anbar Governorate, Iraq Using CMIP6 Models

Zahraa Ali Fadhil [a], Salah L. Zubaidi [a,*], Yousif Almamalachy [b], Mustafa Al-Mukhtar [c], Hatem Hameed Hussein [d], Ruqayah Mohammed [e], Fouad H. Saeed [f], Mawada Abdellatif [g,*], Nadhir Al-Ansari [h]

[a] Department of Civil Engineering, Wasit University, Wasit, 52001, Iraq
[b] National Center for Water Resources Management, Ministry of Water Resources, Baghdad, 10001, Iraq
[c] Civil Engineering Department, University of Technology, Baghdad, Iraq
[d] General Director for Planning and Follow up, Ministry for Water Resources, Baghdad, Iraq
[e] Department of Civil Engineering, Faculty of Engineering, The University of Babylon, Hilla P.O. Box 4, Iraq
[f] Ministry of Water Resources, Baghdad, Iraq
[g] Civil Engineering and Built Environment Department, Faculty of Engineering Technology, Liverpool John Moores University, Liverpool L3 5UX, UK
[h] Department of Civil, Environmental and Natural Resources Engineering, Lulea University of Technology, Lulea, Sweden

ABSTRACT

This study proposes a framework for examining the spatiotemporal characteristics of drought in Anbar Governorate, Iraq, for both historical and future periods, using LARS-WG, five CMIP6 GCMs (SSP245 and SSP585), a Drought Index Calculator, and GIS tools. The Reconnaissance Drought Index (RDI-12) was used to evaluate the spatial-temporal patterns of drought frequency and severity at seven meteorological stations between 1985 and 2015 and between 2021 and 2040. The main conclusions from the study included that LARS-WG performs successfully for climatic factor projection. The general average level of drought expected will be “near-normal dry”, while the maximum drought level expected will be “severely dry”. The near-normal drought category had the highest drought frequency in both the past and future scenarios. The highest values of drought intensity and frequency (severely) were recorded at Rutba Station, with a frequency of 4, and a recurrence rate of 13.33% for the baseline period. For both the first and second future scenarios, Haditha and Anah Stations will report the highest percentage of the moderate drought category (with drought frequency of 4 and recurrence rate of 21.05% for both stations).

Received 27 February 2026; revised 8 May 2026; accepted 8 May 2026.
Available online 19 May 2026

* Corresponding author.
E-mail addresses: Std2022203.Z.A@uowasit.edu.iq (Z. Ali Fadhil), salahlafta@uowasit.edu.iq (S. L. Zubaidi), yogofa@gmail.com (Y. Almamalachy), mmalmukhtar@gmail.com (M. Al-Mukhtar), hatem_altamimy@yahoo.com (H. Hameed Hussein), r.mohammed1@yahoo.com (R. Mohammed), fouadhussein@uowasit.edu.iq (F. H. Saeed), M.E.Abdellatif@ljmu.ac.uk (M. Abdellatif), nadhir.alansari@ltu.se (N. Al-Ansari).

https://doi.org/10.65892/3079-0697.1006

Keywords: Climate change effects, Drought, Emissions scenarios, Iraq, RDI, Spatiotemporal distribution

1. Introduction

Over the past few decades, droughts have become increasingly frequent worldwide due to climate change and global warming [1, 2]. Drought is one of the most destructive natural disasters in the world, and there has been a significant decrease in water availability (relative to its usual levels) over a long period across a large area [3–5]. Drought typically results from a significant reduction in precipitation and an increase in temperature, leading to increased evapotranspiration [6, 7]. Drought conditions have been becoming more severe, especially in arid and semiarid regions such as the Middle East and North Africa (MENA) [8]. Uncertainty about the consequences of climate change on water supplies, along with the increasing demand for water driven by these countries' burgeoning economies and populations, exacerbates the water problem [9].

Jasim and Awchi [1] indicated that Iraq has faced several environmental, economic, and societal effects from the drought. The most notable of them is the unprecedented desertification in some parts of Iraq, the reduction of arable land, and the mass migration of Iraqi rural residents to urban centres. Urbanisation and increases in urban population, the extension of barren land, and decreased vegetation reduce biological productivity, which is associated with cumulative soil erosion by wind and water [10]. Furthermore, the degradation of both soil and vegetation cover caused by desertification has negatively impacted around 70% of arid land. The projected total area of Iraq subject to desertification is 167,000 km^2, equating to 40% of the country's total area of 437,500 km^2 [11].

Prior research have noted the importance of drought indices calculations for various areas of the world. For example, Mohammed and Yimam [12] examined the extent, pattern, and spatiotemporal variability of the meteorological drought in Ethiopia from 1986 until 2019. Drought severity was assessed at 3- and 12-month intervals using the reconnaissance drought index (RDI). Geographic Information Systems (ArcGIS) spatial analyst tool and the inverse distance weighted (IDW) technique were used to estimate the spatial extent of droughts. The results showed that the study area experienced a marked increase in the frequency of drought events from 2008 onwards, compared with previous trends in the 1990s and early 2000s. The trend towards increased dryness in recent years may be a sign of global warming.

Alwan*, et al.* [13] analysed drought in the Middle Euphrates region between 1988 and 2018, tracking both meteorological and agricultural drought conditions using the RDI and Vegetation Condition Index (VCI), respectively, to evaluate drought conditions in cultivation and weather. It was found that the total proportion of drought in the research region had increased compared to a period without drought. From 8% in 1988 and 2000 to 17% in 2018, the percentage of places that did not experience drought fluctuated. The region's severe and extreme drought classifications had the highest ratio, followed by mild and moderate droughts. Throughout the area, particularly in its western and southern sections, the dry season is dominant.

Furthermore, Bahrami*, et al.* [14] assessed the spatiotemporal characteristics of drought in Iran using standardised RDI (RDIst) from 1967 to 2014 at 40 synoptic weather stations and reported an increasing prevalence of drought conditions. A negative trend in the computed RDIst was observed at 90% of the stations across all seasons, suggesting that drought has been increasing over time. Winter showed a significant positive trend across all time ranges in 45% of the stations under study. The findings also indicated that the biggest portion of the research area was affected by a moderate drought.

Recent studies have shown that the negative effects of droughts are expected to worsen in the future due to the expanding global population and rising water demand [15]. These reasons make it economically and socially essential to research how climate change affects drought, mainly in arid and semiarid zones. To close this gap, we intend to provide a thorough spatiotemporal analysis of meteorological drought changes in the western region of Iraq in the short to medium term. In this context, this study seeks to achieve the following objectives: 1) To predict minimum and maximum temperature and precipitation data by using the Long Ashton Research Station Weather Generator (LARS-WG) (Eq. (8)) model for future periods (2021–2040) using seven meteorological stations and using five global climate models (GCMs) to increase certainty and two shared socio-economic pathways (SSPs), SSP245 and SSP585. 2) To use the Drought Indices Calculator (DrinC) program for calculating drought severity and frequency using RDI at the 12-month timescales under each climate change scenario in the future period in western Iraq. 3)To estimate the spatial and temporal variability of drought and draw maps by using ArcGIS's spatial analyst tool and the IDW method, and analyse the results. 4) To provide helpful information to the authorities, stakeholders, and insurance services for facing drought events and minimise localised losses in the short to medium term (2021–2040).

2. Data and methodology

2.1. Description of the case study region and data sources

As one of Iraq's largest provinces, Anbar covers about 137,808 km^2, accounting for almost 32% of the country's total area of 437,072 km^2. Roughly 1.3 million people are living there [16]. Located in western Iraq, Anbar Province covers the Western Plateau, which accounts for 55% of the nation's total area. Geographically, it is located between latitudes 34°24'54" and 34°11'6" North and longitudes 40°28'12" to 41°25'48" East [17].

The province is known for its semiarid climate, marked by minimal precipitation and wide temperature swings between day and night and between summer and winter. Wintertime lows of 0°C or lower are common, while summer temperatures soar beyond 50°C [18]. As a dry region with limited rainfall, Al-Anbar experiences particularly severe drought, which adversely affects the quantity and quality of water resources [19]. The lack of meteorological data in emerging nations is a major problem because of disruptions like terrorism and war that have intermittently plagued Iraq for decades. Thus, satellite data proved to be an accurate replacement for this investigation.

To estimate future weather conditions, daily precipitation and minimum and maximum temperature data from the National Aeronautics and Space Administration (NASA) were utilised for each of the seven research stations for the period 1985–2015. The NASA data were used effectively in recent studies [20, 21]. Table 1 lists the seven meteorological stations, whose locations are depicted in Fig. 1.

Table 1. Details of the meteorological stations.

Station	Longitude	Latitude	Elevation (m asl)
RAMADI	43.19	33.27	91
HEET CITY	43.75	33.633	59
RUTBA	40.17	33.02	689
HADITHA	42.48	34.2	177
NUKHAIB	42.15	32.02	328
ALQAEM	41.01	34.23	233
ANAH	41.57	34.22	282

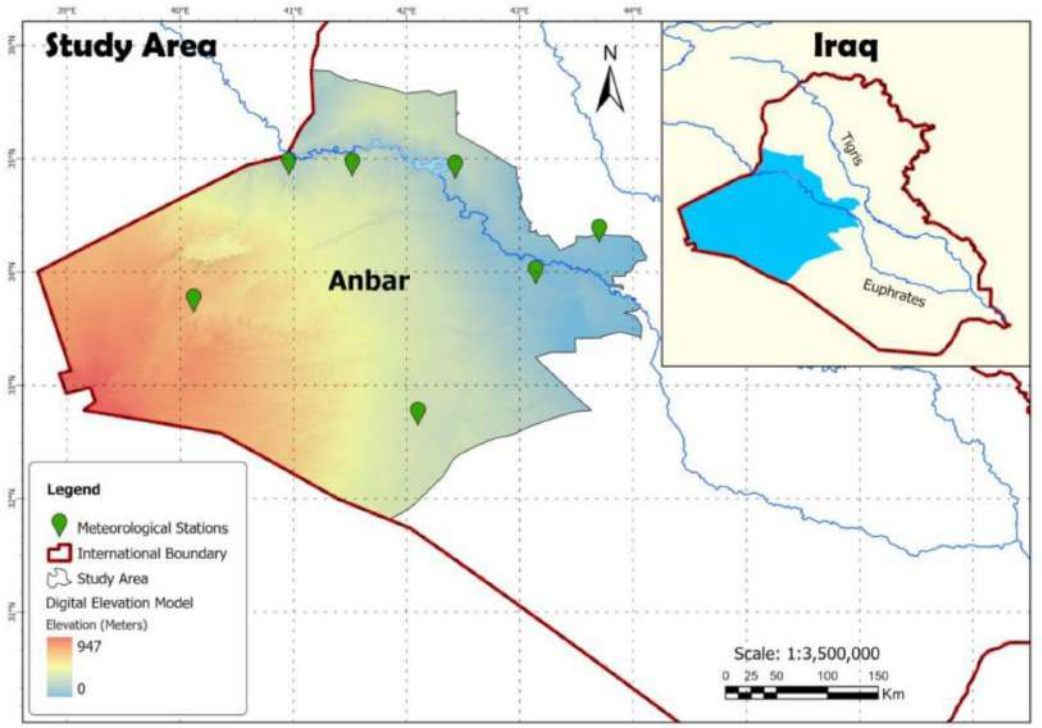

Fig. 1. Spatial distribution of selected stations in the west of Iraq.

2.2. Estimation of evapotranspiration

Several computational methods have been employed to evaluate the reference or Potential Evapotranspiration (PET), which can be categorised as analytical techniques (based on climate variables), hydrological or water-balance techniques, and empirical estimates [22]. The first group, used only in laboratories, consists of material analyses. In contrast, in the second category, the processes of transpiration and evaporation are explained using mathematical relationships centred on the primary climatological elements of mass transfer and energy balance. In this category, two well-known examples are the Penmane-Monteith and Priestley-Taylor equations. Finally, because of their low data needs, empirical methods—which are mostly based merely on temperature—have typically been the most popular solution. However, they suffer from the major drawback of being typically site-specific (depending on local climate) and frequently requiring calibration. This category includes the equations of Thornthwaite, Bleney Criddle, and Hargreaves. We chose PET methods for this research, which fall within the last group (i.e., empirical estimation methods), because they only utilise actual temperature data.

The PET estimate was calculated using the Hargreaves approach, which is considered well-suited for studying climate change and can be used as the primary instrument for estimating PET across numerous climatic settings, including arid and semiarid regions [23]. This has been confirmed by several studies of water resources, including those conducted by [24] and [25]. Mohammed and Scholz [23] also showed a correlation between the Hargreaves method and the best results that approximated the Food and Agriculture Organisation Penman-Monteith method's full equation.

2.3. RDI computation

The DrinC for estimating RDI was used in this study, as shown in Fig. 2 Tigkas, *et al.* [26]. The RDI (a general meteorological index for assessing drought) depends on PET and cumulative precipitation (P). Three forms are available to express the RDI: initial (RDI αk), standardised (RDIst), and normalised (RDIn). The initial formula employed is the aridity index (αk), which is computed on a monthly, seasonal, or annual basis. In a reference period of k (months), as follows:

$$\alpha_k^{(i)} = \frac{\sum_{j=1}^{k} P_{ij}}{\sum_{j=1}^{k} PET_{ij}}, \; i = 1\,(1)\,N \text{ and } j = 1\,(1)\,k \tag{1}$$

Where Pij and PETij represent rainfall and potential evapotranspiration for the j-th month of the i-th year, respectively, and N denotes the number of available years. Across various locations and reference periods, the values of αk showed satisfactory fit to both the lognormal and gamma distributions [27].

By fitting a log-normal probability density function to the provided frequency distribution of αk, the following equation may calculate the standardised form of RDIst:

$$RDI_{st}^{(i)} = \frac{y^{(i)} - \bar{y}}{\hat{\alpha_y}} \tag{2}$$

where y(i) represents $\ln(\alpha_k^{(i)})$, $\bar{y}$ is its arithmetic mean and $\hat{\alpha_y}$ is its standard deviation, according to Tigkas [27]. The standardised form of RDI_{st} can be computed by utilising the equation shown below to fit a log-normal probability density function to the given αk frequency distribution.

$$g(x) = \frac{1}{\beta^{\alpha}\Gamma(\alpha)} x^{\alpha-1} e^{\frac{-x}{\beta}}, \text{ for } : x > 0 \tag{3}$$

Where $\alpha > 0$ is a shape factor, $\beta > 0$ is a scale factor, $x > 0$ is the amount of rainfall, and the gamma function, $\Gamma(\alpha)$, is defined as follows:

$$\Gamma(\alpha) = \int_0^{\alpha} y^{\alpha-1}\, e^{-y} dy \tag{4}$$

To fit a distribution to data, α and β must be estimated in the following ways:

$$\alpha = \frac{1}{4A}\left(1 + \sqrt{1 + \frac{4A}{3}}\right) \tag{5}$$

$$\beta = \frac{\bar{X}}{\alpha} \tag{6}$$

Where

$$A = \ln(\bar{x}) - \frac{\sum \ln(x)}{n} \tag{7}$$

$$G(x) = \int_0^{x} g(x)\, dx = \frac{1}{\beta^{\alpha}\Gamma(\alpha)} \int_0^{x} x^{\alpha-1} e^{\frac{-x}{\beta}} dx \tag{8}$$

A rainfall distribution may contain zeros, which is the cumulative probability. Since the gamma function is undefined for x = 0, the function that might be utilised is:

$$H(X) = q + (1 - q)\,G(X) \tag{9}$$

Where G(x) is the cumulative probability of the incomplete gamma function, and q is the probability of zero precipitation.

The RDIst can be used as a global index, because it offers values categorised into specified drought classifications. When comparing RDIst readings to the area's normal circumstances, positive values indicate wet periods, while negative values indicate dry periods. When RDIst values are lower, drought occurrences become more severe. There are four different classes of drought severity: mild ($-0.5 < \text{RDIst} < -1.0$), moderate ($-1.0 < \text{RDIst} < -1.5$), severe ($-1.5 < \text{RDIst} < -2.0$), and extreme ($\text{RDIst} < -2.0$) [28].

RDI is computed in reference periods of 3, 6, 9, and 12 months for a hydrological year. This suggests that the RDI is not like other drought indices, but rather is produced for specific reference periods. It could focus on the fact that the RDIst is not significantly affected by the PET calculation method; hence, temperature-based methods, such as those of Hargreaves and Samani [29], may be sufficient to generate accurate RDI estimates [30]. The RDI can be computed over a variety of time periods, and traditional drought classifications can be used to interpret the results (Table 2). The latter is especially important in strategic management, as it makes results understandable to non-experts, thereby speeding up the decision-making process. In this research, monthly rainfall and temperature data from seven meteorological stations in western Iraq were utilised. On a

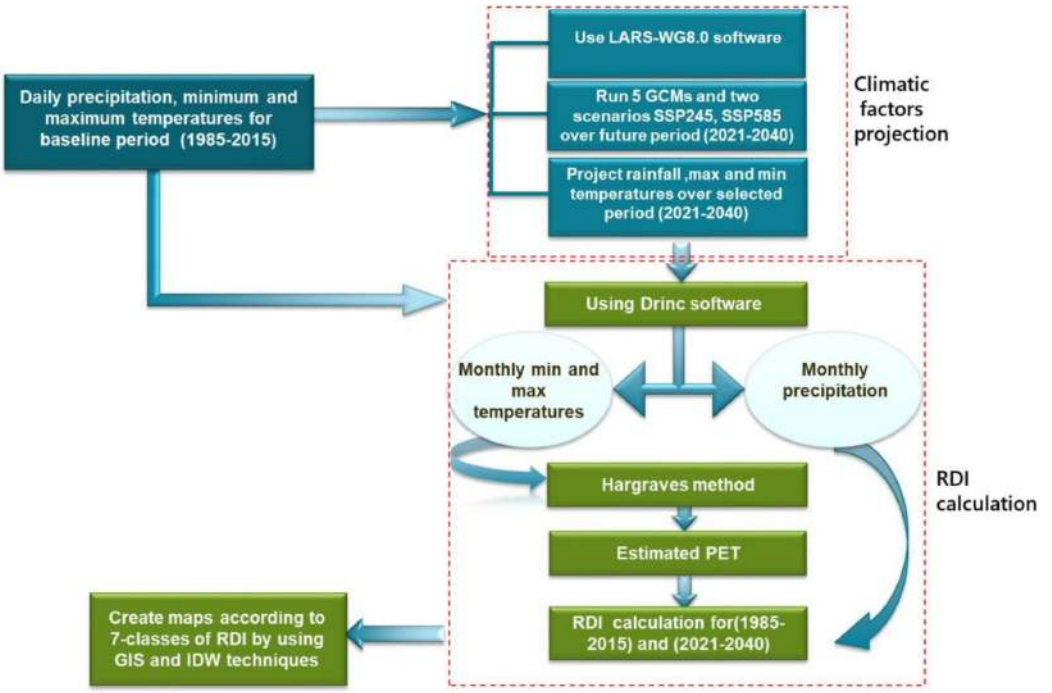

Fig. 2. Flow chart of study methodology.

Table 2. Classification of drought according to the RDIst value.

No.	RDIst range	Drought classes
1	2 or more	Extremely wet
2	1.5 to 1.99	Very wet
3	1 to 1.49	Moderately wet
4	0.99 to −0.99	Near normal
5	−1 to −1.49	Moderately dry
6	−1.5 to −1.99	Severely dry
7	−2 and less	Extremely dry

monthly time scale, RDI values were calculated for 12 months (1985–2015) and for the future period (2021–2040).

2.4. Mapping spatial-temporal distribution of drought incidence

Recently, many studies have generated and used maps of drought severity to indicate and understand particular areas affected by associated droughts. In this study, DrinC software produced RDI values, which were then entered into ArcGIS 10.8.2 to create maps of drought severity for the research zone at 12-month intervals. RDI time-series values from each meteorological station were interpolated using the IDW technique to determine the spatial-temporal extent of droughts in the research area. The methodology used in this study is summarised in Fig. 2.

3. Results

3.1. Calibration and validation of LARS-WG program

The LARS-WG program was calibrated and validated for the stated area using 31 years (1985–2015) of daily historical rainfall, maximum temperature, and minimum temperature data from seven selected stations. The model's capacity to scale down GCMs in the study region was assessed using statistical criteria, such as the Kolmogorov-Smirnov (K-S) test and p-values.

The assessment results show that the LARS-WG model performs very well at predicting daily temperatures and precipitation for the study area, with performance ranging from very good to perfect across all 7 local stations. Table S1 reveals the tests for the minimum temperature for Heet Stations. This indicates that it is a good choice for conducting impact studies on climate change in the MENA region. The reliable performance of the model is in line with results from studies conducted in other parts of the world, which adds to the confidence in the model's use as a downscaling tool in this research, as reported in Europe [31], North America [32], and Asia [33].

3.2. Projection results

The weather generator effectively downscales and forecasts daily temperatures and precipitation for seven local stations based on calibration and validation analyses. LARS-WG was used to project daily climate data from 2021 to 2040 using five GCMs (ACCESS-ESM1-5, CNRM-CM6-1, HadGEM3-GC31-LL, MPI-ESM1-2-LR, and MRI-ESM2-0) under two emission scenarios (SSP245 and SSP585). Using the mean ensemble of GCMs reduces uncertainty and GCM biases [34]. The mean ensemble of GCMs is the most cautious approach to risk management and also produces more precise projections of the future.

The experiment's goals were to identify the distribution of drought-affected areas, discuss the effects of drought in western Iraq, and analyse the frequency and spatial distribution of drought. The daily minimum, maximum, and rainfall readings were converted to monthly values. The readings were then arranged according to the hydrological year from October to September. The PET was determined utilising the Hargreaves method in the DrinC program. Finally, the RDIst was calculated for each year from 2021 to 2040 and transformed into a frequency of severity for the 12 months. It was then converted into a frequency percentage.

This section discusses the frequency analysis of drought occurrence based on the drought classifications derived from RDI values shown in Table 2. The table divides the frequency distribution of the RDI-7 values into 7 categories. Consequently, seven categories emerged from the predicted and actual data (i.e., SSP245 and SSP585): near normal, moderate drought, severe drought, extreme drought, moderately wet, very wet, and extremely wet. For example, the frequency of drought events during the baseline period is shown in Table 3. The near-normal category had the highest drought frequency for both the baseline and future periods.

The frequency percentage of drought for each category was expressed as the ratio of the number of events in this category at each station to the total number of drought events. Table 4 presents the procedures used to calculate the drought frequency percentage for the baseline period at Ramadi Station, as an example. Up to this point, each previous analysis was conducted individually on each selected location. The spatial-temporal distributions of observed and projected drought severity in the study location are shown in Figs. 3 to 7. The data were spatially analysed using ArcGIS 10.8.2 software and Python coding. Using the IDW method, all projected and observed variables are spatially interpolated over the research region and mapped into different classes.

Table 3. Drought frequency (RDI) in seven stations, 1985–2015.

RDI class		Extremely wet	Very wet	Moderately wet	Near normal	Moderately dry	Severely dry	Extremely dry
Station No.	Station Name	2.00 or More	1.50 to 1.99	1.00 to 1.49	0.99 to –0.99	–1.00 to –1.49	–1.50 to –1.99	–2 or Less
1	RAMADI	0	3	2	19	2	3	1
2	HEET	0	0	8	18	0	3	1
3	RUTBA	0	2	2	22	0	4	0
4	HADITHA	0	2	1	23	3	0	1
5	NUKHAIB	0	0	6	17	4	3	0
6	ALQAEM	1	2	0	23	3	0	1
7	ANAH	1	2	0	21	5	0	1

Table 4. Procedures followed to calculate drought frequency percentage for the baseline period of Ramadi station.

Classification	Frequency	Percentage
Severity	Oct-Sept	Oct-Sept
Extremely wet	0	0.00
Very wet	0	0.00
Moderately wet	0	0.00
Near normal	30	100.00
Moderately dry	0	0.00
Severely drought	0	0.00
Extremely drought	0	0.00
Total	30	100

The maps were created according to the classifications given in Table 2. They consisted of both observed and projected RDI under the two emission scenarios (SSP245 and SSP585). The legend displays nine classes of drought incidence with a range of 0–90 for the RDI. The spatial-temporal distribution of drought severity in the research zone for the extremely dry class, showing the frequency distribution of RDI classes over a 12-month time scale. It can be observed that one class emerged from the RDI percentage frequency in the observed and projected periods for both scenarios, SSP245 and SSP585, ranging from 0 to 10 and covering 100% of Anbar's total area. This homogeneity shows a lack of spatial fluctuation, rendering a graphical representation unnecessary.

For illustrative purposes, the RDI for severely dry was mapped over the 12-month time scale, as shown in Fig. 3. Generally, the map of observed percentage frequency of RDI

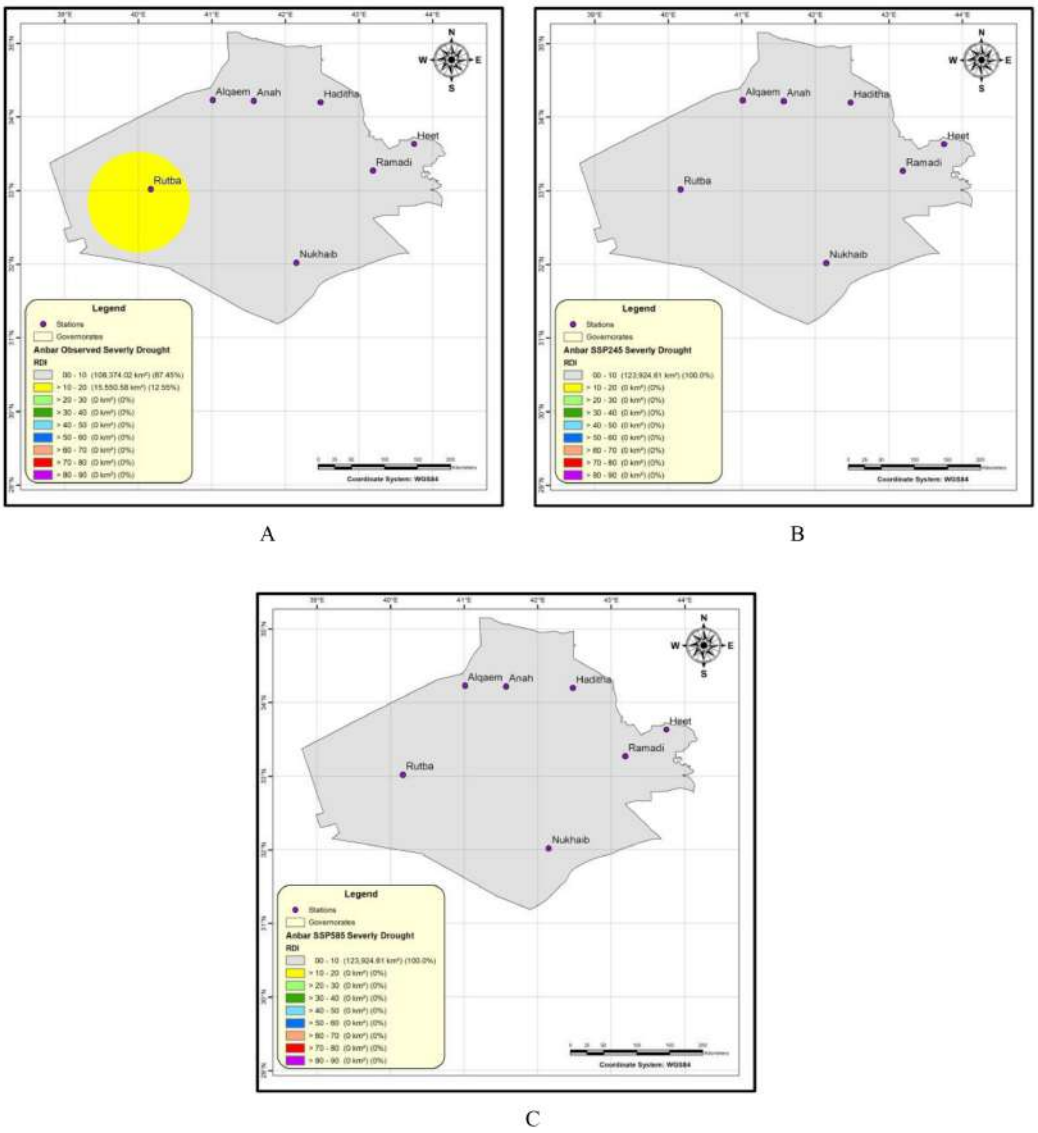

Fig. 3. The spatial-temporal distribution map of drought severity for severely dry category in the research region.

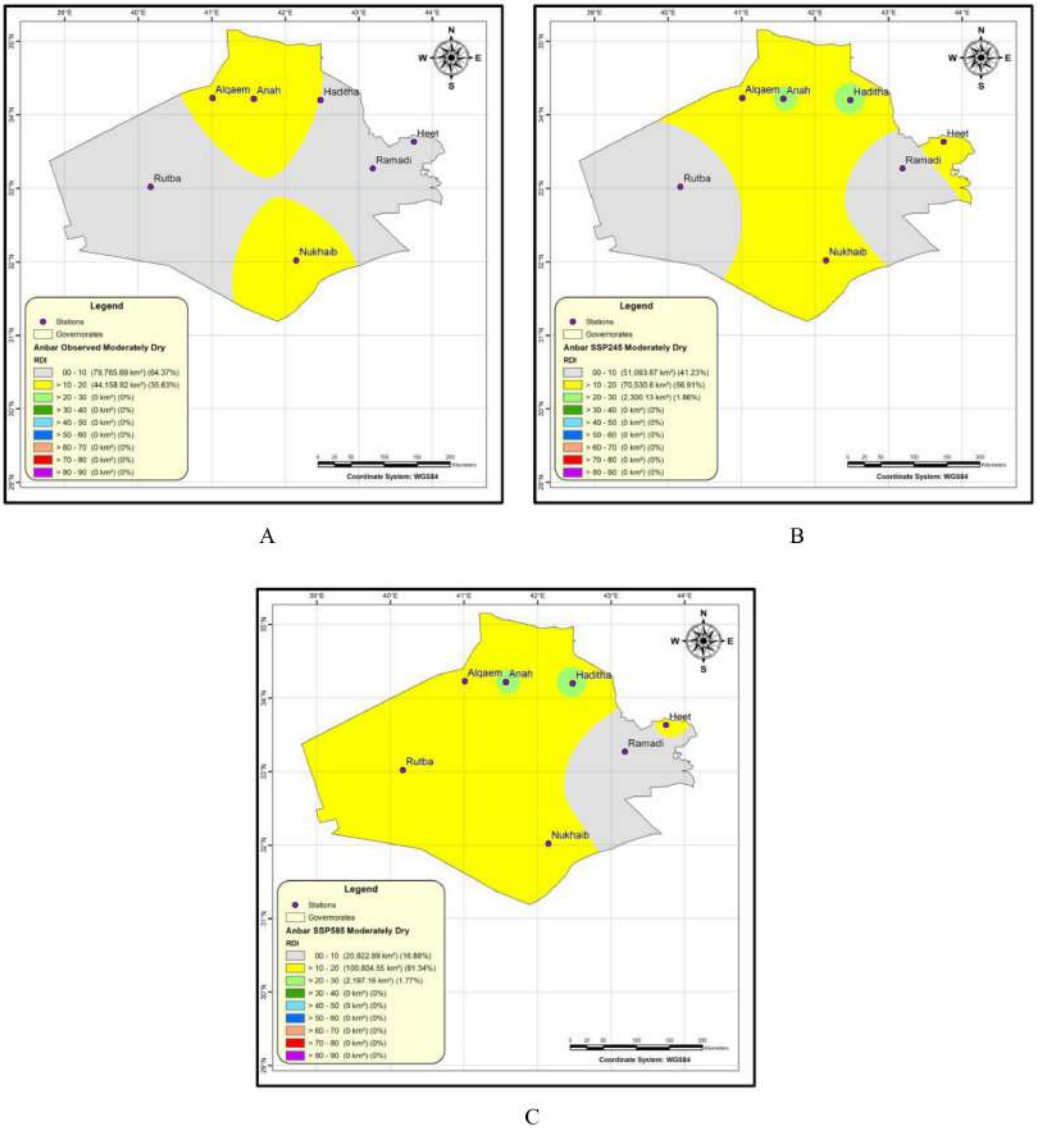

Fig. 4. The spatial-temporal distribution map of drought severity for moderately dry category in the research region.

shows a single dominant class (0–10). The percentage frequency of RDI for the severely dry category is expected to shift from class (10–20) to class (0–10) in both future maps for Rutba Station, indicating a lower likelihood of drought in this area. Considering the future of both SSPs, the percentage frequency of RDI ranges from 0 to 10 for all seven stations.

As shown in Fig. 4, the research area's moderately dry class has a spatial-temporal distribution map of drought severity over the 12 months. The observed data showed a percentage frequency of RDI ranging from 0 to 20. The dominant class (0–10) covers the majority (64.37%) of the selected area. In contrast, Alqaem, Anah, and Alnukhaib had RDI percentages ranging from 10–20, collectively representing 35.63% of the region's total area. In the first scenario (SSP245), the percentage frequency of RDI ranged from 0 to 30. The expected dominant class (10–20) will cover 56.91% of Anbar's total area. The class (0–10) will be represented 41.23%. This category is likely to appear in Rutba

and Ramadi Stations, while Haditha and Anah will appear in the category (20–30) and represent 1.86% of the total area. In the second scenario, SSP585, the class (10–20) will be increased, representing 81.34% of the total area. Ramadi Station will appear in class (0–10) and represent 16.88% of the area. The category (20–30) is likely to account for 1.77% of the total area.

The spatial-temporal patterns of drought over 12 months for a class near normal are depicted in Fig. 5. The RDI values from 7 stations during the research period were used to extrapolate the regional patterns of drought episodes. The frequency of drought in the observed data map ranged from 50 to 80. As shown in the figure, there are three classes: (50–60), (60–70), and (70–80). Class (70–80) is considered the dominant class and represents 53.46% of the region's total area. Class (60–70) accounted for 39.46%, while Alnukhaib Station had the lowest class (50–60) at 7.04%.

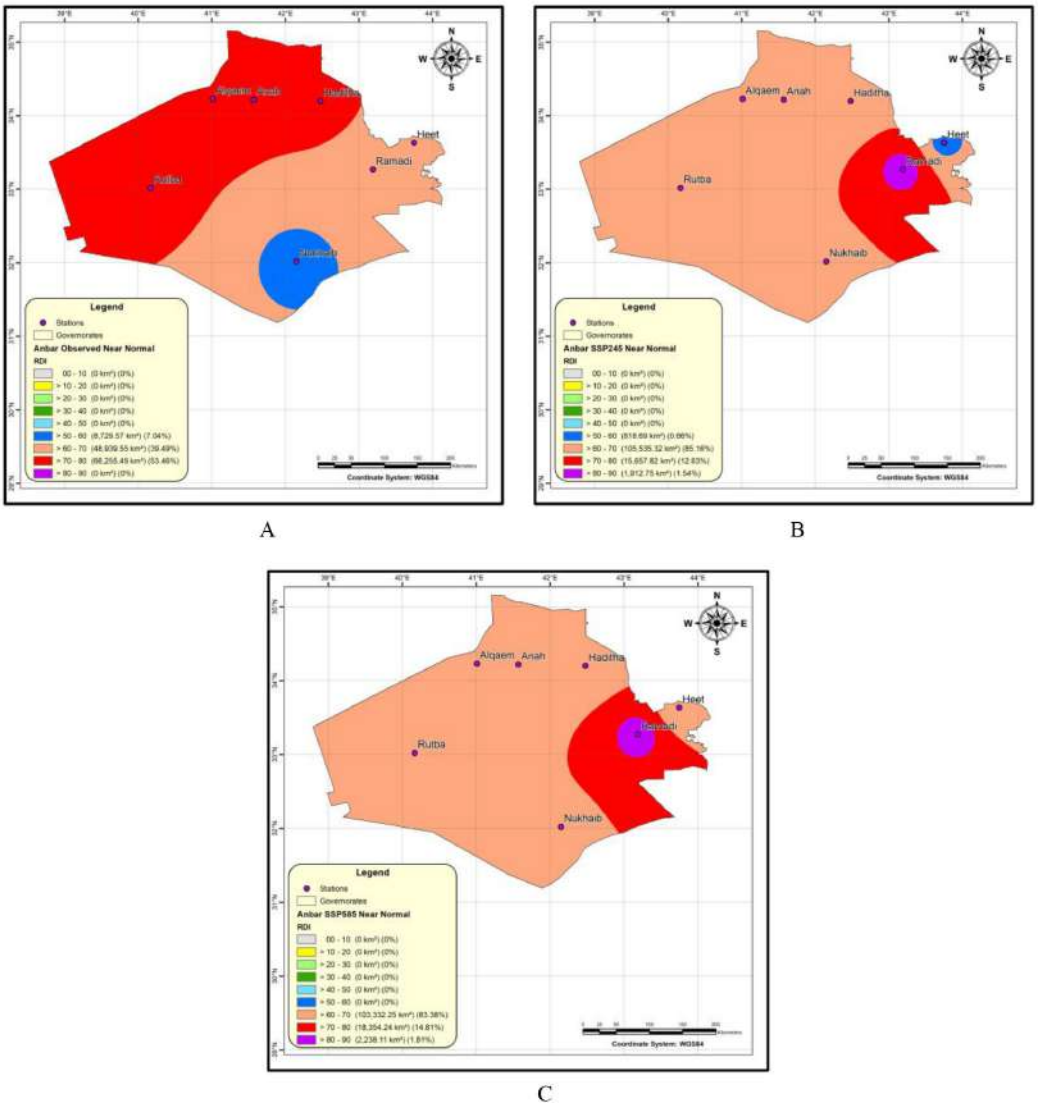

Fig. 5. The spatial-temporal distribution map of drought severity for near normal category in the research region.

In the first scenario (SSP245), the percentage frequency of RDI ranged from 50 to 90. The class (60–70) percentage will likely increase and become the dominant category, accounting for 85.16% of Anbar's total area. In contrast, the class proportion (50–60) is anticipated to drop to 0.66%. Additionally, the class proportion (70–80) will likely drop to 12.63%. We observe that a new class has emerged in Ramadi Station, accounting for 1.54% of the entire region. For the SSP585, the RDI frequency percentile range is 60–90. The findings in this case were close to the first scenario. The class (70–80) will be increased to represent 14.81% of the total area. Furthermore, there was a rise in the class (80–90), accounting for 1.81% of the whole region's area. The class (60–70) will experience a 1.78% drop compared to the initial scenario.

Fig. 6 depicts the spatial-temporal distribution of 12-month drought severity in the research area for the moderately wet class. The percentage frequency of RDI was distributed

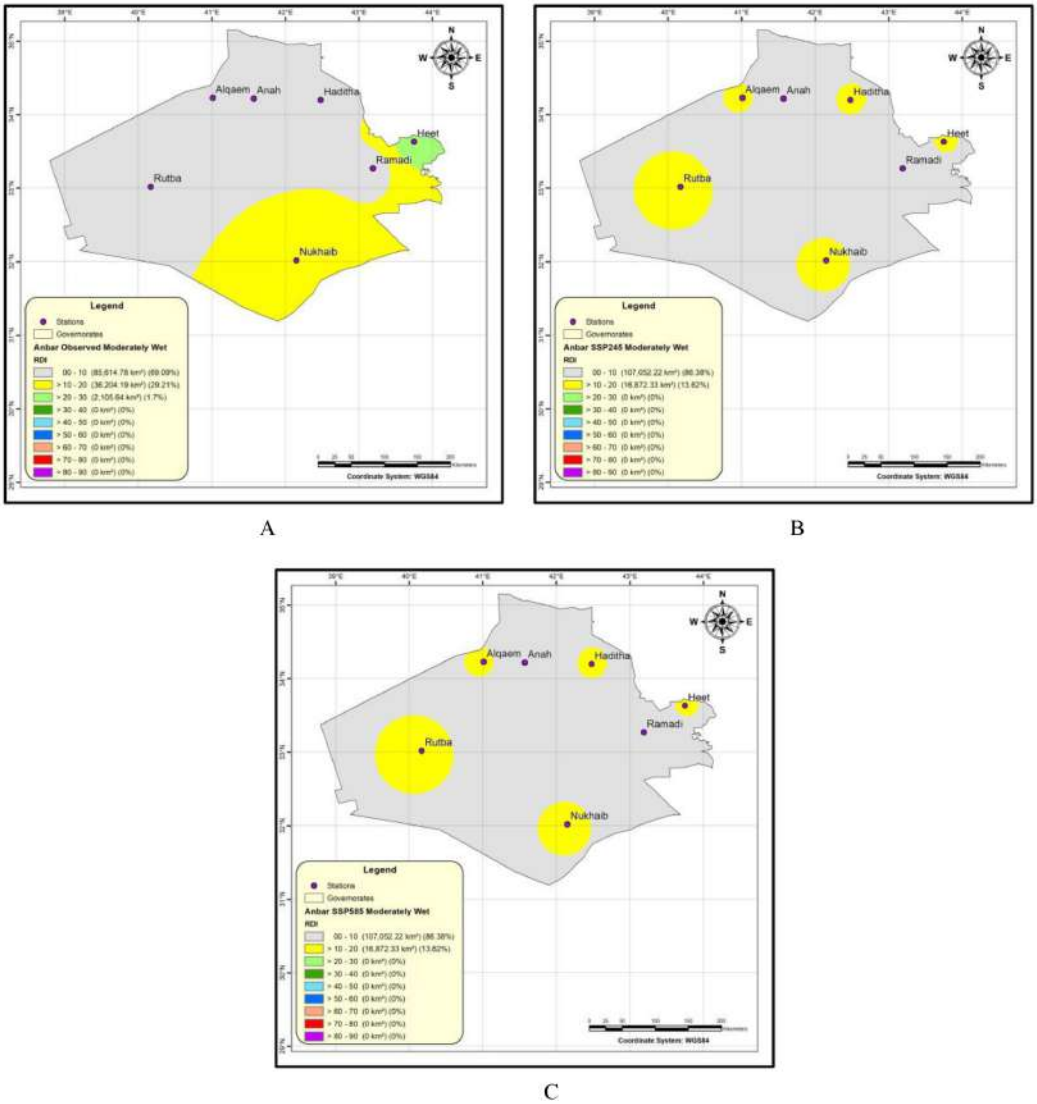

Fig. 6. The research region's spatial-temporal distribution map of drought severity for the moderately wet category.

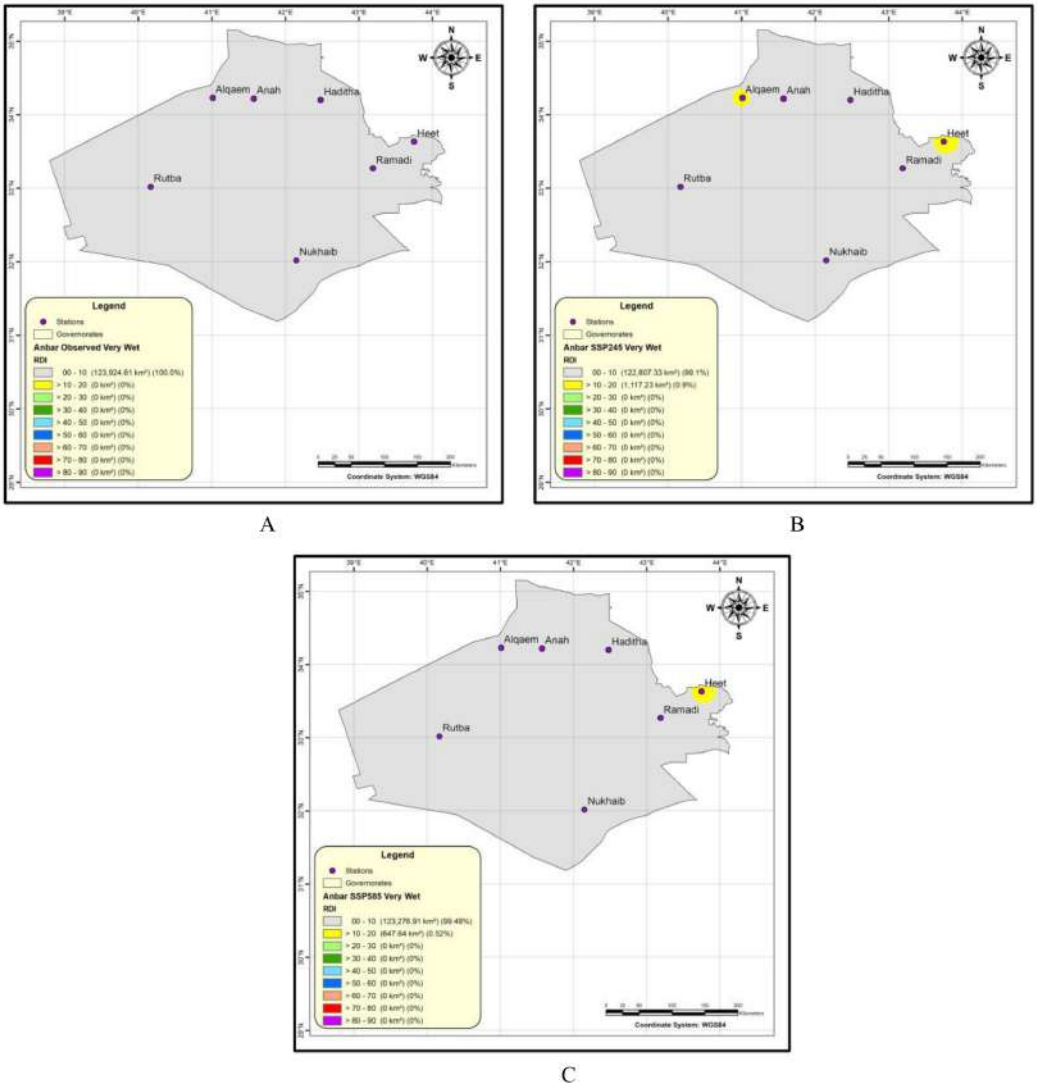

Fig. 7. The research region's spatial-temporal distribution map of drought severity for the very wet category.

across three classes: (0–10), (10–20), and (20–30). Class (0–10) has the highest percentage for observed, SSP245, and SSP585 scenarios, with (69.09%), (86.38%), and (86.38%), respectively. The observed data showed a 29.21% percentage for class (10–20). This class's percentage will be reduced to 13.62% in both the first and second scenarios. The highest frequency of RDI was in the moderately wet class at Heet Station in the observed map, where it occurred at 1.7% in the class (20–30).

Fig. 7 shows the projected and observed maps for the very wet category. The three maps are nearly identical, except for the Heet and Alqaem Stations, which display the class (10–20) rather than (0–10) in the future maps. The outcomes of the two scenarios indicate that Heet is likely to experience heavy floods.

Finally, the spatial-temporal distribution of drought severity in the research zone for the extremely wet class shows the frequency of RDI classes over a 12-month time scale. It can be observed that one class emerged from the RDI percentage frequency in the observed

and projected periods for both SSP245 and SSP585 scenarios, ranging from 0 to 10 and covering 100% of Anbar's total area. This homogeneity shows a lack of spatial fluctuation, rendering a graphical representation unnecessary.

4. Discussion

This investigation of spatial-temporal patterns of drought in western Iraq used the LARS-WG (Eq. (8)) model with 5 GCMs under 2 SSPs to forecast the daily climate variables. To calibrate and validate the LARS-WG program, baseline data spanning 1985–2015 were utilised. After the calibration and validation of the LARS-WG program, daily climatic variables were projected, and the multi-GCM models' ensemble mean was computed for each variable.

After that, the daily minimum and maximum temperature and rainfall readings were converted to monthly values. The readings were arranged from October to September based on the hydrological year. In the DrinC program, the PET was computed utilising the Hargreaves approach. Finally, the RDIst was calculated over 12 months, and the frequency and spatial distribution of drought were analysed for actual and projected data (i.e., SSP245 and SSP585). Subsequently, the IDW technique and ArcGIS 10.8.2 were used to understand better fluctuations among stations in the measured and projected spatial-temporal distribution of 12-month drought severity in the research region.

The outcomes show that drought occurrences in western Iraq presented spatial and temporal variations. Interestingly, the near-normal category was the highest drought category, as shown in Fig. 5; the frequency of RDI rates ranged from 50 to 90 at nearly all stations across the research area for both future scenarios. The highest values of intensity and frequency for the severe drought category were recorded at Rutba Station during the baseline period, followed by Anah and Haditha Stations during the future period, as shown in Figs. 3 and 4. The highest RDI value was 1.86 in 2013 at Rutba Station, in the severely dry category, during the baseline period, when the drought frequency was 4, and its percentage was 13.33%. Drought severity and distribution are mainly influenced by complex factors, including climatic, anthropogenic, and natural variables, which disproportionately affect arid regions [35]. As such, spatial variations in drought intensity and frequency made the country highly vulnerable to climate change and its detrimental implications. Therefore, local and regional collaboration is required to sustain shared resources more effectively and adapt to changing climatic conditions.

Haditha and Anah Stations recorded the highest percentage of moderate drought category for both the first and second future scenarios (i.e., SSP245 and SSP585). The frequency of drought was 4, and its frequency percentage was 21.05% at both stations. In these regions, drought is exacerbated by the soil's geological nature: it consists mainly of sandy soils that are continually eroded by wind. Also, their capacity to retain water, especially precipitation water, was negatively affected by the high porosity of these soils. These areas also lack surface water resources; their only water supply is highly saline water from a few wells [13].

Low rates of both the moderate wet and very wet categories were observed across all areas, as shown in Figs. 6 and 7. The percentage of RDI frequency ranged from 0 to 10 in each instance, reflecting the low annual rainfall volume. Heet Station was an exception in displaying the class (10–20) rather than the class (0–10) in future maps; the outcomes of the two scenarios indicate that Heet Station is likely to experience severe flooding. Regarding the extreme categories, no difference was observed between Figs. 3 and 7. It is apparent that extremely low rates of both extreme wet and extreme drought conditions prevail, as the percentage of RDI frequency ranged from 0 to 10 at all stations and across both scenarios.

In summary, the findings showed that the general average level of drought expected will be near-normal dry, while the maximum drought level will be severely dry. Our findings are in line with previous literature, which reported considerable fluctuations in drought recurrence and severity across different sites in Iraq [36, 37]. The MENA's droughts are positively correlated with the phenomenon of climate change, which will cause higher temperatures, decreased precipitation and runoff, and increased water scarcity. These factors will lead to a downturn in agriculture, a worsening economy, rising poverty, mass migration, and political unrest [38]. Increasing agricultural water-use efficiency and productivity, improving the monitoring and management of groundwater resources, and international cooperation to share rivers that cross multiple countries are among the most important measures available to combat the effects of drought [39].

Regarding the outcomes of this search, one limitation of this study is that it utilises satellite data rather than observed data, as the latter is unavailable for 7 stations during the baseline period due to successive waves of conflict, terrorism, and political instability and insecurity in Iraq. Despite these limitations, this study contributes to addressing the egregious shortage of studies on meteorological drought in Iraq and other countries in the MENA region. This study is the first to use RDI to address these problems in the western region of Iraq.

5. Conclusion

This research aims to evaluate the meteorological drought in western Iraq in terms of its frequency, severity, trend, and spatial-temporal patterns by employing RDI to generate drought data for a 12-month timescale, from seven sites for the baseline period of 1985–2015 and the projected period of 2021–2040. The investigation's salient conclusions were as follows: 1) The RDI frequency percentage map (00–10 class) is the most common (100%) for the extremely dry and extremely wet categories throughout the baseline period, and it will likely remain the most common for SSP245 and SSP585 from 2021 to 2040 as well. Also, the very wet category has the same condition as the former categories to some extent. 2) The RDI frequency percentage map (00–10 class) covers about 87.45% of the area identified as severely dry throughout the baseline period. It will likely cover the entire research area for both SSPs in the future. Rutba Station is expected to experience more severe drought than other stations. 3) The drought frequency percentage maps showed that the SSPs were worse than the observed maps for a moderately dry category. In general, the scenario SSP585 was the worst. Anah and Hadith Stations are expected to achieve a high frequency percentage. The drought frequency was 4, and its recurrence rate was 21.05% for both stations. Also, the same thing for a moderately wet category. Generally, both scenarios are expected to get the same frequency percentage and spatial distributions for RDI classes.

Further research could benefit from expanding upon the present findings by investigating the following: 1) using a different satellite data source, for example, Google Earth Engine. 2) One possibility is to use another statistical downscaling technique, and 3) an additional drought index for studying the spatial and temporal variability of meteorological drought.

Supplementary material

Supplementary material available at: https://wsjet.uowa.edu.iq/cgi/viewcontent.cgi?filename=0&article=1006&context=journal&type=additional&preview_mode=1.

Acknowledgements

We would like to express our gratitude to the National Centre for Water Resources Management (Iraq) for generously providing the required equipment during the course of this research and for dedicating valuable time to its development.

Conflict of interest

The authors declare that they have no conflict of interest.

Funding

This research did not receive any funding.

Data availability

The data that support the findings of this study are available on request from the corresponding author.

CRediT authorship contribution statement

Zahraa Ali Fadhil: Formal analysis, Investigation, Methodology, Validation, Writing - original draft, Writing - review & editing.
Salah L. Zubaidi: Methodology, Conceptualization, Project administration, Supervision, Software, Writing - review & editing.
Yousif Almamalachy: Data curation, Investigation, Software, Resources, Visualization.
Mustafa Al-Mukhtar: Data curation, Methodology, Software, Resources.
Hatem Hameed Hussein: Methodology, Software, Writing - review & editing.
Ruqayah Mohammed: Methodology, Software, Writing - review & editing.
Mawada Abdellatif: Methodology, Software, Writing - review & editing.
Nadhir Al-Ansari: Methodology, Software, Resources, Visualization.

Abbreviations

MENA	Middle East and North Africa
RDI	Reconnaissance Drought Index
ArcGIS	Geographic Information Systems
IDW	Inverse Distance Weighted
VCI	Vegetation Condition Index
RDIst	Standardised Reconnaissance Drought Index
LARS-WG	Long Ashton Research Station Weather Generator
GCMs	Global Climate Models
SSPs	Shared Socio-Economic Pathways
DrinC	Drought Indices Calculator
NASA	National Aeronautics and Space Administration
PET	Potential Evapotranspiration

P	Precipitation
RDI αk	Initial Reconnaissance Drought Index
RDIn	Normalised Reconnaissance Drought Index
K	Months
K-S	Kolmogorov-Smirnov Test

References

1. Jasim AI, Awchi TA. Regional meteorological drought assessment in Iraq. Arabian Journal of Geosciences. 2020;13(7). doi:10.1007/s12517-020-5234-y.
2. Vicente-Serrano SM, Quiring SM, Peña-Gallardo M, Yuan S, Domínguez-Castro F. A review of environmental droughts: Increased risk under global warming? Earth-Science Reviews. 2020;201:102953. doi:doi.org/10.1016/j.earscirev.2019.102953.
3. Tsakiris G, Pangalou D, Vangelis H. Regional Drought Assessment Based on the Reconnaissance Drought Index (RDI). Water Resources Management. 2006;21(5):821–833. doi:10.1007/s11269-006-9105-4.
4. Zhang Q, Li Q, Singh VP, Shi P, Huang Q, Sun P. Nonparametric Integrated Agrometeorological Drought Monitoring: Model Development and Application. Journal of Geophysical Research: Atmospheres. 2018;123(1):73–88. doi:10.1002/2017jd027448.
5. Xu D, Zhang Q, Ding Y, Zhang D. Application of a hybrid ARIMA-LSTM model based on the SPEI for drought forecasting. Environmental Science and Pollution Research. 2022;29(3):4128–4144. doi:10.1007/s11356-021-15325-z.
6. Dorjsuren M, Liou Y-A, Cheng C-H. Time Series MODIS and in Situ Data Analysis for Mongolia Drought. Remote Sensing. 2016;8(6). doi:10.3390/rs8060509.
7. Alawsi MA, Zubaidi SL, Al-Bdairi NSS, Al-Ansari N, Hashim K. Drought Forecasting: A Review and Assessment of the Hybrid Techniques and Data Pre-Processing. Hydrology. 2022;9(7). doi:10.3390/hydrology9070115.
8. Tigkas D, Tsakiris G. Early estimation of drought impacts on rainfed wheat yield in Mediterranean climate. Environmental Processes. 2015;2:97–114. doi:10.1007/s40710-014-0052-4.
9. Masood T, Sonntag P. Industry 4.0: Adoption challenges and benefits for SMEs. Computers in Industry. 2020;121. doi:10.1016/j.compind.2020.103261.
10. Sulaiman SO, Al-Ansari N, Shahadha A, Ismaeel R, Mohammad S. Evaluation of sediment transport empirical equations: case study of the Euphrates River West Iraq. Arabian Journal of Geosciences. 2021;14(10):825. doi:10.1007/s12517-021-07177-1.
11. Sulaiman SO, Kamel AH, Sayl KN, Alfadhel MY. Water resources management and sustainability over the Western desert of Iraq. Environmental Earth Sciences. 2019;78(16):495. doi:10.1007/s12665-019-8510-y.
12. Mohammed Y, Yimam A. Analysis of meteorological droughts in the Lake's Region of Ethiopian Rift Valley using reconnaissance drought index (RDI). Geoenvironmental Disasters. 2021;8(1). doi:10.1186/s40677-021-00183-1.
13. Alwan IA, Ziboon AT, Khalaf AG, Pham QB, Anh DT, Khedher KM. Monitoring agricultural and meteorological drought using remote sensing. Arabian Journal of Geosciences. 2022;15(2). doi:10.1007/s12517-021-09407-y.
14. Bahrami M, Bazrkar S, Zarei AR. Spatiotemporal investigation of drought pattern in Iran via statistical analysis and GIS technique. Theoretical and Applied Climatology. 2020;143(3-4):1113–1128. doi:10.1007/s00704-020-03480-1.
15. Dierauer JR, Zhu C. Drought in the twenty-first century in a water-rich region: modeling study of the Wabash River Watershed, USA. Water. 2020;12(1):181. doi:10.3390/w12010181
16. Awadh SM. A preliminary assessment of the geochemical factors affecting groundwater and surface water quality around the rural communities in Al-Anbar, Western Desert of Iraq. Environmental Earth Sciences. 2018;77(3). doi:10.1007/s12665-018-7262-4.
17. Noon AM, Ahmed HGI, Sulaiman SO. Assessment of Water Demand in Al-Anbar Province- Iraq. Environment and Ecology Research. 2021;9(2):64–75, doi:10.13189/eer.2021.090203.
18. Sulaiman SO, Kamel AH, Sayl KN, Alfadhel MY. Water resources management and sustainability over the Western desert of Iraq. Environmental Earth Sciences. 2019;78(16). doi:10.1007/s12665-019-8510-y.
19. Jasim MA, Shafri HZM, Hamedianfar A, Sameen MI. Land transformation assessment using the integration of remote sensing and GIS techniques: a case study of Al-Anbar Province, Iraq. Arabian Journal of Geosciences. 2016; 9(15). doi:10.1007/s12517-016-2697-y.

20. Kadhim Tayyeh H, Mohammed R. Analysis of NASA POWER reanalysis products to predict temperature and precipitation in Euphrates River basin. Journal of Hydrology. 2023;619. doi:10.1016/j.jhydrol.2023.129327.
21. Oliazadeh A, Bozorg-Haddad O, Mani M, Chu X. Developing an urban runoff management model by using satellite precipitation datasets to allocate low impact development systems under climate change conditions. Theoretical Applied Climatology. 2021;146:675–687, doi:10.1007/s00704-021-03744-4.
22. Zarei AR, Mahmoudi MR. Evaluation of changes in RDI st index effected by different Potential Evapotranspiration calculation methods. Water Resources Management. 2017;31:4981–4999. doi:org/10.1007/s11269-017-1790-7.
23. Mohammed R, Scholz M. Impact of climate variability and streamflow alteration on groundwater contribution to the base flow of the Lower Zab River (Iran and Iraq). Environmental Earth Sciences. 2016;75(21). doi:10.1007/s12665-016-6205-1.
24. Ramkar P, Yadav SM. Spatiotemporal drought assessment of a semi-arid part of middle Tapi River Basin, India. International Journal of Disaster Risk Reduction. 2018;28:414–426. doi:10.1016/j.ijdrr.2018.03.025.
25. Tigkas D, Vangelis H, Tsakiris G. An Enhanced Effective Reconnaissance Drought Index for the Characterisation of Agricultural Drought. Environmental Processes. 2017;4(S1):137–148. doi:10.1007/s40710-017-0219-x.
26. Tigkas D, Vangelis H, Tsakiris G. DrinC: a software for drought analysis based on drought indices. Earth Science Informatics. 2014;8(3):697–709. doi:10.1007/s12145-014-0178-y.
27. Tigkas D. Drought characterisation and monitoring in regions of Greece. European water. 2008;23(24):29–39.
28. Tigkas D, Vangelis H, Tsakiris GJSotTE. Drought and climatic change impact on streamflow in small watersheds. 2012;440:33–41. doi:org/10.1016/j.scitotenv.2012.08.035.
29. Hargreaves GH, Samani ZA. Estimating potential evapotranspiration. Journal of the irrigation Drainage Division. 1982;108(3):225–230. doi:10.1061/JRCEA4.0001390.
30. Vangelis H, Tigkas D, Tsakiris G. The effect of PET method on Reconnaissance Drought Index (RDI) calculation. Journal of Arid Environments. 2013;88:130–140. doi:10.1016/j.jaridenv.2012.07.020.
31. Trnka M, Balek J, Semenov MA, Semeradova D, Belinova M, Hlavinka P, Olesen JE, Eitzinger J, Schaumberger A, Zahradnicek P, Kopecky D, Zalud Z. Future agroclimatic conditions and implications for European grasslands. Biologia plantarum. 2021;64:865–880. doi:10.32615/bp.2021.005.
32. Gitau MW, Mehan S, Guo T. Weather Generator Effectiveness in Capturing Climate Extremes. Environmental Processes. 2018;5(S1):153–165. doi:10.1007/s40710-018-0291-x.
33. Sheikhbabaei A, Hosseini Baghanam A, Zarghami M, Pouri S, Hassanzadeh E. System Thinking Approach toward Reclamation of Regional Water Management under Changing Climate Conditions. Sustainability. 2022;14(15). doi:10.3390/su14159411.
34. Ishaque W, Osman R, Hafiza BS, Malghani S, Zhao B, Xu M, Ata-Ul-Karim ST. Quantifying the impacts of climate change on wheat phenology, yield, and evapotranspiration under irrigated and rainfed conditions. Agricultural Water Management. 2023;275:108017. doi:10.1016/j.agwat.2022.108017.
35. Chang S, Chen H, Wu B, Nasanbat E, Yan N, Davdai B. A Practical Satellite-Derived Vegetation Drought Index for Arid and Semi-Arid Grassland Drought Monitoring. Remote Sensing. 2021;13(3). doi:10.3390/rs13030414.
36. Al-Quraishi AMF, Gaznayee HA, Crespi M. Drought trend analysis in a semi-arid area of Iraq based on Normalized Difference Vegetation Index, Normalized Difference Water Index and Standardized Precipitation Index. Journal of Arid Land. 2021;13(4):413–430. doi:10.1007/s40333-021-0062-9.
37. Gaznayee HAA, Al-Quraishi AMF, Mahdi K, Messina JP, Zaki SH, Razvanchy HAS, Hakzi K, Huebner L, Ababakr SH, Riksen M, Ritsema C. Drought Severity and Frequency Analysis Aided by Spectral and Meteorological Indices in the Kurdistan Region of Iraq. Water. 2022;14(19). doi:10.3390/w14193024.
38. Mathbout S, Lopez-Bustins JA, Martin-Vide J, Bech J, Rodrigo FS. Spatial and temporal analysis of drought variability at several time scales in Syria during 1961–2012. Atmospheric Research. 2018;200:153–168. doi:10.1016/j.atmosres.2017.09.016.
39. Gleick PH. Water, drought, climate change, and conflict in Syria. Weather, climate,and society. 2014;6(3):331–340, doi:doi.org/10.1175/WCAS-D-13-00059.1.